JOURNAL OF SOLID STATE CHEMISTRY **129,** 206–213 (1997)
ARTICLE NO. SC967214

Ti XAS of a Novel Cs–Ti Silicate

N. J. Hess,[1] M. L. Balmer, and B. C. Bunker

Pacific Northwest National Laboratory, Richland, Washington 99352

and

S. D. Conradson

Los Alamos National Laboratory, Los Alamos, New Mexico 87545

Received August 12, 1996; accepted November 6, 1996

Ti XANES and EXAFS were performed to determine the coordination environment of Ti in several Ti oxide standards with known structures and two unknowns with $CsTiSi_2O_{6.5}$ composition, one amorphous and one fully crystalline. Analysis of both the XANES and EXAFS data of the unknowns indicate that Ti^{4+} is 5-fold coordinate in $CsTiSi_2O_{6.5}$ and that the site is highly distorted. Plots of intensity versus the energy of a Ti pre-edge feature result in the separation of 6-, 5-, and 4-fold coordinate Ti into three distinct regions. EXAFS and XANES data show that the Ti coordination environment for the amorphous and crystalline $CsTiSi_2O_{6.5}$ samples is the same indicating that the Ti coordination environment forms early in the crystallization process. Preliminary measurements at the Cs *K*-edge EXAFS on the same samples shows that the Cs coordination environment is different for the amorphous and the crystalline $CsTiSi_2O_{6.5}$ samples suggesting that the Cs coordination environment forms late in the crystallization process.

INTRODUCTION

Crystalline silicotitanates (CSTs) have been proposed as ion exchange materials for the removal of Cs and Sr from high level nuclear waste streams (1). Currently, Cs and Sr are released from the loaded traditional ion exchange resins by elution and then incorporated into solid waste forms. Reprocessing by elution is not possible with CSTs; however, another strategy is to directly incorporate the loaded CST into a solid waste form, for example, borosilicate glass logs, by melting. In addition, recent studies (2) have demonstrated that some cesium silicotitanates can be directly transformed to a crystalline material isostructural with pollucite ($CsAlSi_2O_6$) at temperatures well below those required for formation of borosilicate glass. The Ti-substituted pollucite, $CsTiSi_2O_{6.5}$, has leach rates that lower than that for the borosilicate glass, generates lower volumes of high level waste, and due to the low processing temperatures, the Cs losses due to volatilization during processing are extremely low. This application and the potential use of other silicotitanate zeolites as catalytic materials has spurred interest in determining the coordination environment of Ti in these novel materials.

X-ray absorption spectroscopy experiments were performed to determine the oxidation state and coordination environment of Ti^{4+} where it is substituted for Al^{3+} in the cesium aluminosilicate pollucite, $CsAlSi_2O_6$. In pollucite, both Al and Si occupy tetrahedral sites and the tetrahedra share apexes to form an open three dimensional network. The cesium atoms occupy the largest cavities in the network. The substitution of Ti^{4+} for Al^{3+} requires some mechanism for charge compensation, perhaps the presence additional oxygen as suggested by neutron powder diffraction results (3). Recently, questions of Ti valence and coordination in zeolitic materials have been addressed using the analysis of the XANES and EXAFS spectra (4–9). Some researchers have reported some difficulty in determination of Ti coordination number (4, 8, 10). In this work, several Ti standards, a Cs standard and two $CsTiSi_2O_{6.5}$ samples prepared with different heat treatments were analyzed. The intensity and energy of a pre-edge feature in the Ti-XANES spectra allowed separation of the 6-, 5-, and 4-fold coordinate Ti samples into distinct regions. These results were supported by analysis of the EXAFS data once the EXAFS spectra had been corrected for self-absorption effects.

DATA COLLECTION

The analyzed samples included standards: TiO_2-anatase and rutile, $BaTiSi_3O_9$, $NaTiSi_4O_{11}$, ETS-4, Na_2TiSiO_5,

[1] To whom correspondence should be addressed.

0022-4596/97 $25.00

$K_2Ti_2O_5$, Ba_2TiO_4, $Ba_2TiSi_2O_8$, $CsAlSi_2O_6$-pollucite, and $CsAlTiSiO_4$, and two unknowns of $CsTiSi_2O_{6.5}$ synthesized at PNNL. The structure and the Ti coordination environment of the standards have been reported in the literature. However for $K_2Ti_2O_5$ there is a discrepancy in the reported metrical parameters and what is calculated based on the space group, lattice dimensions and fractional coordinates for this structure. Based on the metrical parameters, the Ti is reported as occupying a trigonal bipyramidal structure (11, 12). Based on the space group and fractional coordinates, Ti in $K_2Ti_2O_5$ resides in a severely distorted square-pyramidal polygon. The square pyramidal coordination environment is consistent with the recent structure refinement of $K_2Ti_2O_5$ using the results from Raman spectroscopy and powder diffraction (13). The microporous silicate, ETS-4 (9), was chosen as a standard because of the occurrence of Ti in a three-dimensional silica network, an environment that is thought to be analogous to the Ti environment in the $CsTiSi_2O_{6.5}$. The structure of ETS-4 is thought to be similar to the zeoloite, Ti-β, and has only been determined by XAS analysis (18). The unknown, $CsTiSi_2O_{6.5}$ A, was sintered at 700°C and is amorphous using X-ray powder diffraction while, $CsTiSi_2O_{6.5}$ B, which was sintered at 800°C, is fully crystalline.

The XAS data were collected at the Stanford Synchrotron Radiation Laboratory during six experimental runs in the 2-year period 1994–1996. To allow data collection at both the Ti-edge at 6,965 eV and the Cs *K*-edge at 36,000 eV, a wiggler line endstation, beamline 4-2, using Si[220] and Si[400] crystals was selected. Additional data at the Ti *K*-edge was collected on a bending magnet line, beamline 2-3, using Si[220] crystals. Data were collected in fluorescence using either a 13-element Ge array detector or, in later experiments, a Lytle detector. In both arrangements the beam path was flooded with He to reduce the intensity attenuation of the low energy X-rays by air at the Ti *K*-edge. To maximize flux the spectra were collected with the two monochrometer crystals fully tuned and harmonic rejection at Ti *K*-edge was accomplished using critical angle reflection off of a Rh-coated mirror. No method of harmonic rejection was employed at the high energy of the Cs *K*-edge. All data were collected at liquid nitrogen temperatures.

All the samples were analyzed in powder form. The Na_2TiSiO_5 and $K_2Ti_2O_5$ samples were heated treated at 400°C for 12 hr prior to analysis to drive off water. The amount of powders required to result in an absorption unit of one was calculated, weighed-out, and thoroughly mixed with small amount of glucose using a mortar and pestle. The resulting mixture was pressed into a slot of a sample holder using a hydraulic press. The sample holder was then sealed with Kapton tape mounted on the cold finger of a liquid nitrogen cryostat. The cryostat was placed in the beam path so that the plane of the samples was at 45° to the incident beam. A titanium metal foil was also mounted on the sample holder and was used to calibrate the X-ray energy periodically during the fluorescence measurements. Data at the Cs *K*-edge data were internally calibrated by setting the inflection point to 36,005.0 eV. In almost all cases, multiple scans were collected and averaged to increase the signal to noise ratio.

DATA ANALYSIS

The XAS spectra were split into two regions for data analysis. The XANES, or pre-edge region, extending from approximately 50 eV below the absorption edge to 100 eV above the edge, and the EXAFS region, at energies above the absorption edge. The XANES region generally contains direct information about the oxidation state of the absorber. In the case of Ti the XANES region is especially rich and can be used to extract information on bond length and site symmetry (14, 15). However, much of the interpretation of the XANES data is based on an empirical association of features that are observed in well-characterized standards to similar features observed in unknowns.

The data in the EXAFS region is used to extract quantitative information on the number and bond length of coordinating atoms in each coordination sphere. In addition, the chemical identity of the coordinating atoms can be determined. Unlike XANES data analysis, there is a complete theoretical understanding of the EXAFS features (16, 17).

Background subtraction and normalization were performed following standard practice described briefly below. A linear polynomial is fit through the preedge region and extrapolated under the absorption edge. A second polynomial is fit to the EXAFS region and extrapolated to the absorption edge. At approximately 5 to 20 eV above the edge, the extrapolated preedge is set to zero value and the resulting vertical difference between these two extrapolated lines is normalized to one. As a result the intensity of the EXAFS oscillations is on a per atom basis. A two or three segment polynomial spline through the EXAFS region was determined by the minimization of the amplitude of the Fourier transform region from 1 to 3 Å. The normalized absorption spectra was subtracted from the spline and weighted by k^3.

Ti-XANES

The Ti-XANES region was fit using a commercially available fitting package GRAMS386. The preedge region from 4950 to 4990 eV was fit using a linear combination of Gaussian curves. For anatase, which displayed the most complex XANES spectra, eight Gaussian curves were required. Most of the other XANES spectra were significantly simpler and required fewer Gaussian components. To represent the Ti *K*-edge jump a single Gaussian curve was fixed

at 4990 eV with an amplitude of 1 ± 0.05 for all spectra. As found by Waychunas (14), the resulting Gaussian curves could be grouped into two regions; on the low energy tail of the absorption edge and on the edge itself. The frequency and intensity of the Gaussian features have been correlated with the symmetry, coordination number and bond length of the first coordination sphere. No analysis of the Cs XANES was performed because this region is relatively featureless.

EXAFS

The Ti and Cs EXAFS data were simulated and fit with parameterized scattering amplitudes calculated using the FEFF6.0 code developed by Professor John Rehr and coworkers at the University of Washington (16, 17). Several model compounds were created using the FEFF6.0 code and crystallographic data from the literature. From these model compounds, individual scattering paths were parameterized and used to fit the several of the standards and the two unknowns. The fits were made to the unfiltered data. Each fit was evaluated by several methods. First, Fourier transforms were performed over the fitted region to see if results actually fitted features apparent in *r*-space. In addition each scattering path was compared to the residual in *k*-space to be sure there was frequency and node matching. A third method to evaluate the quality of the fit was to Fourier transform each scattering path and compare it to the residual. A fourth method was to perform the fit over several *k*-ranges to determine whether some features were not created by the choice of Fourier transform range. For each shell there are five parameters used in the fit: delta E_0, the scale factor, the number of atoms, the distance, and sigma or the disorder. Two of these, delta E_0 and the scale factor, are determined by fitting the filtered EXAFS of the first oxygen shell of a known reference material, in this case anatase. Delta E_0 and the scale factor are fixed at these values for the remaining samples. The other three parameters, the number of atoms, the distance, and sigma or the disorder are allowed to vary for each shell.

Ti EXAFS

The Ti EXAFS region was fit over the data range from $k = 2.5$ to 10 Å^{-1} except for the data for $K_2Ti_2O_5$ which were fit over the data range from $k = 2.5$ to 9 Å^{-1}. The change in fitting range was necessary because the EXAFS of this sample was perturbed by a large monochrometer glitch at approximately $k = 9.1$ Å^{-1}. The Ti *K*-edge EXAFS over the two fitting ranges for the six samples are shown in Fig. 1. Qualitatively, the EXAFS of all six samples show a general similarity in the periodicity and the node placements of the first two oscillations. At higher *k* values, the similarity of the EXAFS decreases. In addition the signal-to-noise ratio decreases. The amplitude of the anatase EXAFS is appreciably greater than the other samples, especially at high *k*.

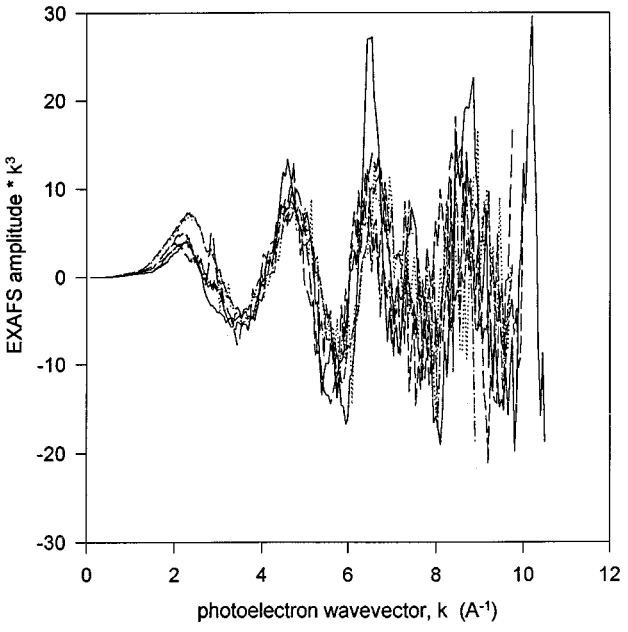

FIG. 1. Ti *K*-edge EXAFS. The EXAFS of the two $CsTiSi_2O_{6.5}$ unknowns are compared to the Ti standards.

The Fourier transforms of the EXAFS data over the fitted *k*-range are presented in Fig. 2. The Fourier transform of the EXAFS is commonly called the radial distribution function,

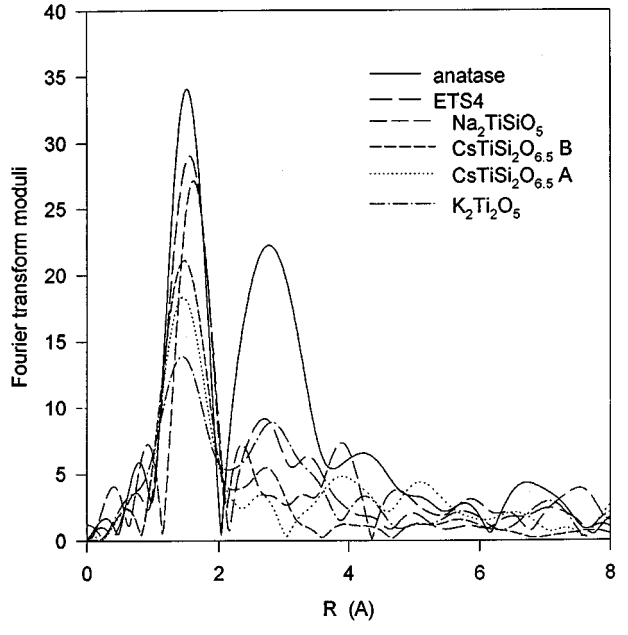

FIG. 2. Radial distribution function at Ti *K*-edge. Fourier transforms were calculated from 2.5 to 10 Å^{-1} using a Gaussian window of 0.5 Å^{-1}. Note that peak positions have not been phase corrected.

or RDF. The RDF gives a more immediate "physical" picture of the EXAFS results because it represents the radial spatial distribution and density of neighboring atoms from the point of reference of the absorbing atom. The first peak in the RDF represents the scattering off Ti nearest neighbor atoms, in this case oxygen. The RDF plot shown in Fig. 2 has not been corrected for the phase shift and the apparent distances are generally shorter by 0.5 to 1.0 Å than those distances determined by fitting the data. At the first level of approximation, a large amplitude can reflect either a large number of atoms or atoms with high atomic number. The amplitude can be diminished in intensity by both static and thermal contributions to the disorder in atomic positions.

Because the focus of this study is on the immediate coordination environment around the Ti atoms, back Fourier transforms were performed around the oxygen shell to remove contributions to the EXAFS from the more distant shells. The amplitude and the real part of the back Fourier transforms are plotted in Fig. 3. The oxygen EXAFS oscillation at anatase exhibits the largest amplitude, in addition the amplitude is uniform across the k-range, indicating that there is minimal disorder in the oxygen positions. The microporous silicate, ETS-4, has the next largest amplitude at low k; however, the amplitude decreases significantly at high k. The decrease in amplitude at k suggests that the disorder in oxygen positions is greater than that found for anatase. Na_2TiSiO_5 oxygen amplitude has lower amplitude at low k than both anatase and ETS-4 but the amplitude does not decrease at high k suggesting that Na_2TiSiO_5 has fewer oxygen nearest neighbors than anatase and ETS-4 but less disorder than ETS-4. The two $CsTiSi_2O_{6.5}$ unknowns and the $K_2Ti_2O_5$ sample have amplitudes that are similar to Na_2TiSiO_5 but their amplitudes diminish dramatically at high K, indicating significant disorder in the oxygen positions. Also apparent in Fig. 3 is the difference in the frequency of the EXAFS oscillations. Generally, higher frequency oscillations reflect longer Ti–O bond lengths. Fits to the back Fourier transform involved a single oxygen shell based on the phase and amplitude functions extracted from FEFF calculations on anatase.

Cs EXAFS

The EXAFS of the Cs K-edge were not analyzed in detail. The objective of the Cs EXAFS study was to determine how the Cs environment compared qualitatively to the aluminosilicate pollucite and whether the Cs environment changed between the two heat treatments for the synthesized samples. The Cs K-edge EXAFS are shown in Fig. 4. Fourier transforms performed over a k-range from $k = 4$ to 10 $Å^{-1}$ are shown in Fig. 5. The first shell consists of scattering amplitude from 10 oxygens at bond lengths of 3.3 to 3.5 Å. The second shell with the largest amplitude consists of scattering paths from both Si and Ti second nearest neighbors. Cs atoms at approximately 4.8 Å dominate the contribution to the third most distant shell. There is striking similarity in the transforms of the Cs environment in

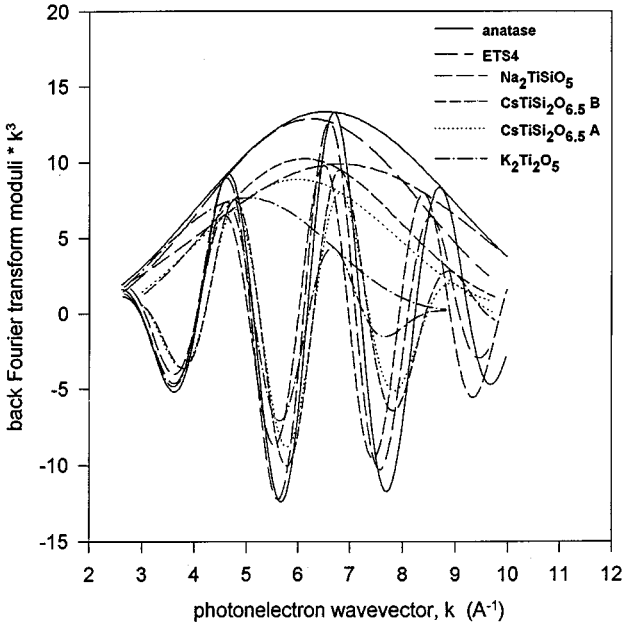

FIG. 3. Back Fourier transform of Ti–O Peak. Back Fourier transforms were calculated for the Ti–O peak centered between 0.8 to 2.1 $Å^{-1}$. The real component of the Fourier transform and the amplitude are plotted.

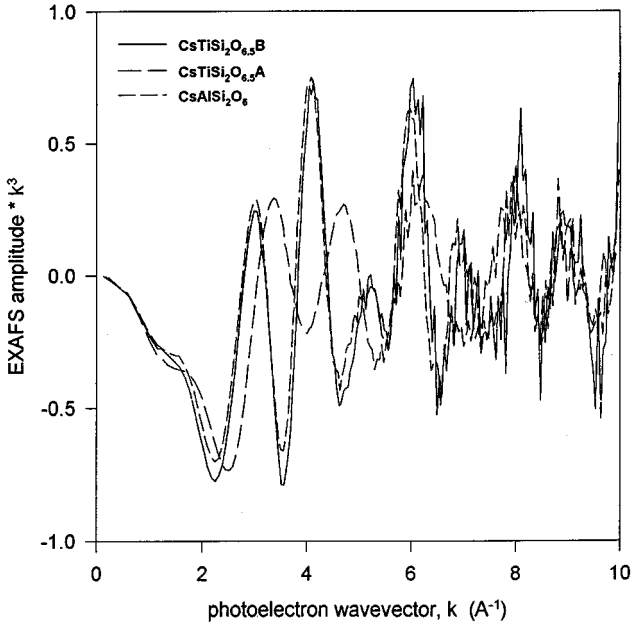

FIG. 4. Cs K-edge EXAFS. The EXAFS of the two $CsTiSi_2O_{6.5}$ unknowns are compared to the Cs standard, $CsAlSi_2O_6$-pollucite.

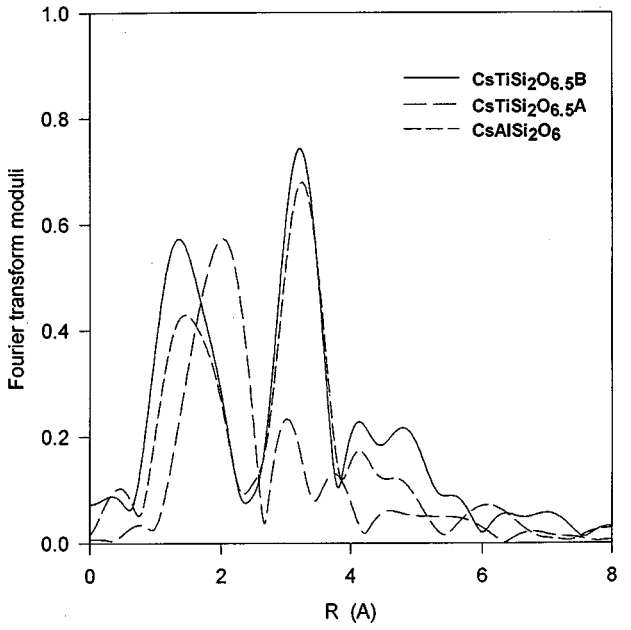

FIG. 5. Radial distribution function at Cs *K*-edge. Fourier transforms were calculated from 4.0 to 12 $Å^{-1}$ using a Gaussian window of 0.5 $Å^{-1}$. Note that peak positions have not been phase corrected.

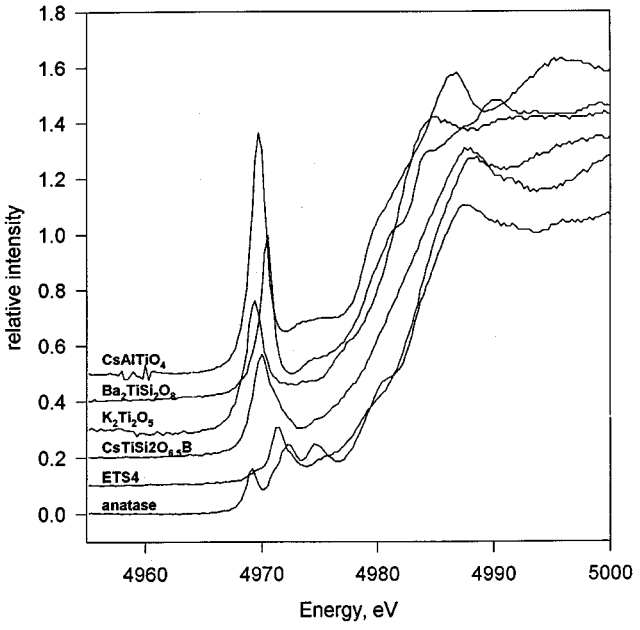

FIG. 6. Ti *K*-edge XANES. The EXAFS of the two $CsTiSi_2O_{6.5}$ unknowns are compared to the Ti standards.

$CsTiSi_2O_{6.5}B$ and the aluminosilicate pollucite $CsAlSi_2O_6$ in even the most distant shell. $CsTiSi_2O_{6.5}A$ only exhibits amplitude in the first shell.

FITTING RESULTS

The Ti *K*-edge XANES region of the samples is shown in Fig. 6. Based on the energy of the absorption edge all of the compounds analyzed contain Ti^{4+}. In addition, two groups of preedge features can be recognized, one group centered at approximately 4970 eV and a second group on the steep slope of the absorption edge. Of these, the second feature in the first group, A2, shows significant variation in intensity and energy relative to the absorption edge from compound to compound. Changes in A2 intensity have been correlated to the amount of distortion from perfect octahedral coordination (14), and the energy of this peak has been correlated with the number of coordinating oxygens. Preedge features on the steep slope of the absorption edge show a strong correlation with Ti–O bond length. The curve-fitting results for anatase Ti-XANES is shown in Fig. 7. Tables 1a and 1b list the fitting results for peak A2 for all samples and for values found in the literature.

The XANES fitting results listed in Table 1 are compared graphically in Fig. 8. Plotting the relative energy versus A2 peak intensity separates the samples into three regions. The samples with six-coordinate Ti have low A2 peak intensity and large relative energy. Samples with five-coordinate span a diagonal of the plot from low relative energy and A2 peak intensity to high relative energy and A2 peak intensity. The four-coordinate Ti samples have low relative energy and high A2 peak intensity. The $CsTiSi_2O_{6.5}$ unknowns fall in the diagonal region representing 5-coordinate compounds.

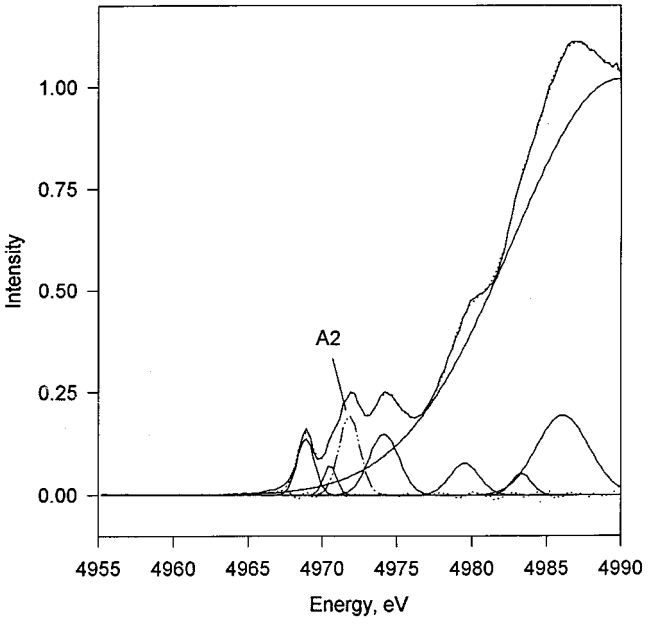

FIG. 7. Gaussian components used in the curve-fit of anatase Ti-XANES. Anatase XANES from 4955 to 4990 eV was fit using a linear combination of 8 Gaussian curves. The preedge feature, A2, displays a systematic shift in intensity and in energy with Ti coordination number.

TABLE 1a
Curve-Fitting Results for Preedge Feature A2

Sample	Intensity	Energy[a] (eV)	Coordination
TiO_2 anatase	0.20	5.5	6
TiO_2 rutile	0.14	5.3	6
Na_2TiSiO_5	0.68	4.2	5
$K_2Ti_2O_5$	0.41	3.8	5
ETS-4	0.19	4.6	5 or 6
$BaTiSi_3O_9$	0.13	4.7	6
$Na_2TiSi_4O_{11}$	0.30	4.5	6
$Ba_2TiSi_2O_8$	0.51	4.1	5
$CsAlTiO_4$	0.83	3.4	4
$CsTiSi_2O_{6.5}B$	0.35	3.4	?
$CsTiSi_2O_{6.5}A$	0.27	3.1	?

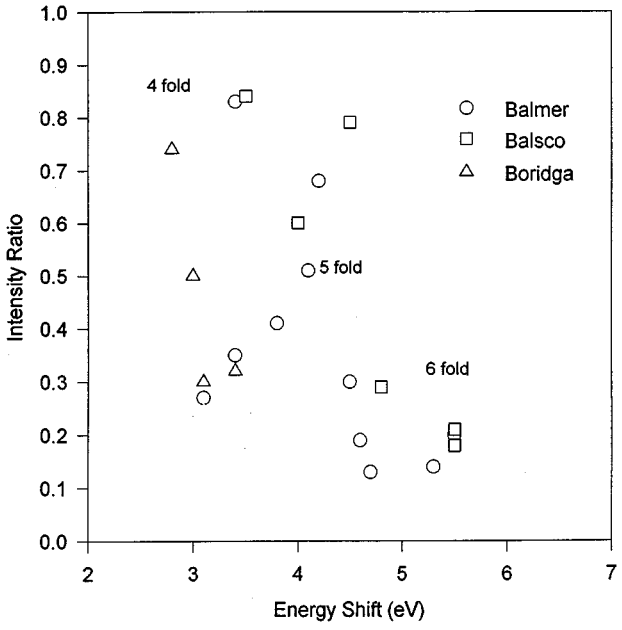

FIG. 8. Plot of the intensity versus energy of Preedge feature A2. Curve-fit results for the Ti standards and unknowns are compared to values found in the literature. Four-, 5-, and 6-coordinate Ti separate into distinct regions of intensity and energy.

The EXAFS fitting results are listed in Tables 2a and 2b for the oxygen coordination shell around Ti. The calculated FEFF Ti–O scattering amplitude was multiplied by a scattering factor of 0.42 in order to generate the six oxygens required for the anatase structure. Typically the FEFF6 code correctly calculates the scattering amplitude so that little correction is needed. A correction of this magnitude suggests that the low energy X-ray fluorescence may have been absorbed by the powder particles themselves, a process called self-absorption. Self absorption can usually be avoided by diluting the sample with a low Z matrix material and grinding the powders to a small particle size. Both techniques were employed in this work. If the scattering geometry is known and the stoichiometry of one standard is known, then self-absorption corrections can be made to the amplitude of the EXAFS oscillations following the procedure of Torger (19). Evaluation of the fitting results to the standards where the coordination environment of Ti is known allows one to gauge the certainty of the results determined for the unknowns and for structural situations were the fitting results are problematic. Therefore, the fitting results for the standards will be discussed in some detail before moving on to the two $CsTiSi_2O_{6.5}$ unknowns.

TABLE 1b
Literature Values for Preedge Feature A2

Sample	Intensity	Energy[a] (eV)	Coordination
TiO_2 anatase[b]	0.21	5.5	6
TiO_2 rutile[b]	0.18	5.5	6
Ramsayite[b]	0.29	4.8	6
Titanyl phthalocyanine[b]	0.79	4.5	5
Fresnoite[b]	0.60	4.0	5
Ba_2TiO_4[b]	0.84	3.5	4
$Ti(OAm)_4$[c]	0.74	2.8	4
$Ti(OPr)_4$[c]	0.50	3.0	4
$Ti(OEt)_4$[c]	0.32	3.4	5
$Ti(OBu)_4$[c]	0.30	3.1	5

[a] Energy relative to E_0 defined as the first inflection point of the absorption edge of Ti foil at 4965 eV.
[b] Data from Ref. 5.
[c] Data from Ref. 18.

The fitting results for the two 6-coordinate standards, anatase and ETS-4, reveal an oxygen shell containing six oxygens at 1.95 Å. Sigma, the disorder parameter, is quite small but consistent with the minor difference between the six Ti–O bond lengths. The fitting results for anatase are in quite good agreement with the metrical parameters and the results for ETS-4 agree well with XAFS results on a similar structure, the zeolite Ti-β (18).

The fitting results for the two 5-coordinate standards, Na_2TiSiO_5 and $K_2Ti_2O_5$, reveal an oxygen shell containing five oxygens at 2.00 Å and 1.95 Å, respectively. As listed in Table 2b, these structures contain one Ti–O bond that is significantly shorter than the four other Ti–O bonds. Such a large difference in bond lengths generally results in a large sigma value. Surprisingly, sigma for the Na_2TiSiO_5 Ti–O shell has zero value. When the EXAFS oscillations for a short Ti–O bond (eg. 1.70 Å) and for the longer 2.0 Å bond length are overlaid in k-space, the oscillations are nearly π out of phase over most of the fitting range. As a result, the two waves beat against each other, interfering destructively. This result suggests that the square pyramidal coordination environment may present a problematic geometry for EXAFS analysis, especially when a limited k-space range is

TABLE 2a
EXAFS Fitting Results for First Oxygen Shell

Sample	Distance[a]	Number[b]	Sigma	r^2
TiO_2-anatase	1.96 ± 0.01	6.0 ± 0.9	0.00 ± 0.00	0.4601
ETS-4	1.99 ± 0.01	5.7 ± 0.9	0.01 ± 0.00	0.5009
Na_2TiSiO_5	2.00 ± 0.01	4.8 ± 0.7	0.00 ± 0.00	0.3360
$K_2Ti_2O_5$	1.95 ± 0.02	5.3 ± 0.9	0.09, fixed	0.5301
$Cs_2TiSiO5B$	1.93 ± 0.01	5.3 ± 0.9	0.07 ± 0.01	0.5161
Cs2TiSiO5A	1.94 ± 0.01	5.4 ± 0.9	0.06 ± 0.02	0.6652

[a] Delta E_0 for Ti–O = 1.0 eV.
[b] Scale factor for Ti–O = 1.00.

used in the fit. The sigma value for the $K_2Ti_2O_5$ structure is quite large and is consistent with the large distribution of Ti–O bond lengths determined for this structure.

The best fits to the two $CsTiSi_2O_{6.5}$ unknowns result in five oxygens at 1.93 Å. This Ti–O distance is consistent with the results of Pei (10) who found that compounds with 5-fold coordinate and Ti had Ti–O bond distances of 1.90 Å or greater whereas 4-fold and 6-fold coordinate and Ti compounds are typified by 1.76 and 1.81 Å and 1.95 to 2.00 Å Ti–O bond lengths, respectively. The similarity of the Ti–O environments for the two $CsTiSi_2O_{6.5}$ compounds is remarkable considering that the powder XRD for these samples indicate that the $CsTiSi_2O_{6.5}$A sample is X-ray amorphous and the $CsTiSi_2O_{6.5}$B sample is fully crystalline. This suggests that the local Ti–O environment forms early in the crystallization sequence of these compounds. Sigma is quite large for both samples indicating that there is significant variability in the Ti–O bond lengths. A comparison of the fitted EXAFS to the back Fourier transforms is shown in Fig. 9.

TABLE 2b
Metrical Parameters for First Oxygen Shell

Standard	Distance		Number
TiO_2-anatase[a]	1.94		4
	1.97		2
Na_2TiSiO_5[b]	1.70		1
	1.99		4
$K_2Ti_2O_5$	1.58	1.67[c]	1
	1.65[d] or 1.91[e]	1.87	1
	1.99	1.99 to 2.08	3
ETS-4[f]	1.94 ± 0.02		5.5 ± 0.5

[a] From Ref. (20).
[b] From Ref. (21).
[c] Distances from Ref. (13).
[d] Distance published by Andersson and Wadsley (11, 12).
[e] Distance calculated using crystallographic data in Andersson and Wadsley (11, 12).
[f] Based on EXAFS from Ref. (18).

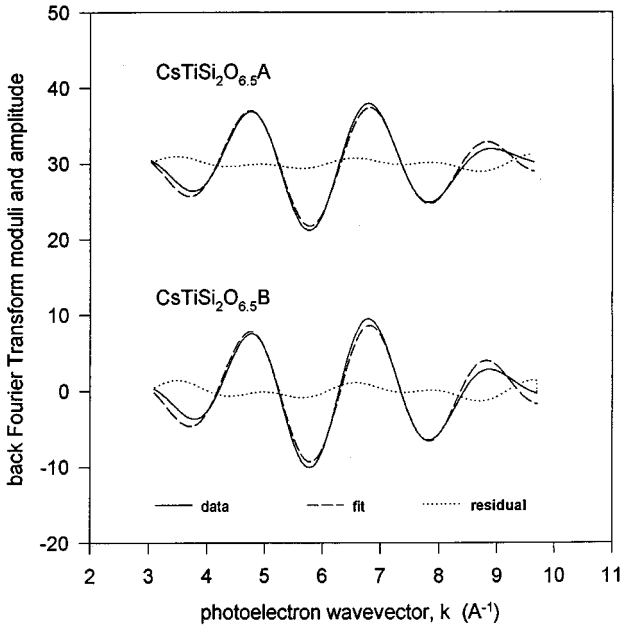

FIG. 9. Comparison of the fit to back-fourier transform for Ti–O. *K*-space comparison of the FEFF fitting results to the back Fourier transforms of the Ti–O shell for the two $CsTiSi_2O_{6.5}$ unknowns.

CONCLUSIONS

Based on the energy of the inflection point of the Ti *K*-edge absorption feature, the oxidation state of Ti in the $CsTiSi_2O_{6.5}$ samples is Ti^{4+}. Analysis of the XANES spectra strongly indicate that the Ti in the two $CsTiSi_2O_{6.5}$ samples is 5-fold coordinate and this result is supported by the analysis EXAFS data. Comparison of the fitting results of the Ti standards to the metrical parameters suggests that once the EXAFS are corrected for self-absorption effects the number of oxygens can be determined. For 5-fold coordinate Ti compounds, a determination of the disorder associated with the Ti–O bond lengths in each structure may not be possible due to destructive interference of EXAFS scattering amplitudes from the short Ti–O bond distance and the longer Ti–O bonds. However, the intensity and energy of a preedge feature in the XANES can be used to separate 4-, 5-, and 6-fold coordinate Ti compounds reliably.

The similarity of the Ti–O environments for the amorphous and fully crystalline $CsTiSi_2O_{6.5}$ samples suggests that the local Ti–O environment forms early in the crystallization sequence for these compounds. This results contrasts with the EXAFS result for the local Cs–O environment. Only the fully crystalline $CsTiSi_2O_{6.5}$ sample showed strong similarity to the aluminosilicate standard pollucite. This suggests that the Cs coordination environment is formed at the latest stages of crystallization, a result that could have significant impact on Cs waste form synthesis.

ACKNOWLEDGMENTS

The authors thank Dr. James Dickinson, Corning Glass Corporation, for providing samples of $Na_2Ti_2Si_2O_9$ and $K_2Ti_2O_5$ and Drs. Farrel Lytle and Glen Waychunas for helpful discussions on data collection and XANES analysis of Ti compounds. This work was performed at Stanford Synchrotron Radiation Laboratory, which is operated by the US Department of Energy, Office of Basic Energy Sciences, Division of Chemical Sciences. Pacific Northwest National Laboratory is operated by Battelle Memorial Institute for the US Department of Energy under Contract DE-AC06-76-RLO 1830.

REFERENCES

1. R. G. Anthony, C. V. Phillip, and R. G. Dosch, *Waste Management* **13,** 503 (1993).
2. M. L. Balmer and B. C. Bunker, Inorganic Ion Exchange Evaluation and Design—Silicotitanate Ion Exchange Waste Conversion, Pacific Northwest National Laboratory Technical Report, PNL-10460, 1995.
3. M. L. Balmer, Q. Huang, W. Wong-Ng, A. Santoro, and B. Roth, Neutron and X-ray diffraction study of the crystal structure of $CsTiSi_2O_{6.5}$, submitted for publication.
4. P. Behrens, H. Felsche, S. Vetter, G. Schulz-Ekloff, N. I. Jaeger, and W. Niemann, *J. Chem. Soc. Chem. Commun.* 678 (1991).
5. T. Blasco, M. A. Camblor, A. Corma, and J. Perez- Pariente, *J. Am. Chem. Soc.* **115,** 11,806 (1993).
6. G. Deo, A. M. Turek, I. E. Wachs, D. R. C. Huybrechts, and P. A. Jacobs, *Zeolites* **13,** 365 (1993).
7. G. Sankar, F. Rey, J. M. Thomas, G. N. Greaves, A Corma, B. R. Dobson, and A. J. Dent, *J. Chem. Soc. Chem. Commun.* 2279 (1994).
8. E. Schultz, C. Ferrini and R. Prins, EXAFS and XANES on Ti-containing zeolite Y, *Jpn. J. Appl. Phys.* **32,** 490 (1993).
9. S. M. Kuznicki, K. A. Thrush, F. M. Allen, S. M. Levine, M. M. Hamil, D. T. Hayhurst, and M. Mansour, *in* "Synthesis of Microporous" (M. L. Ocelli, Ed.), Vol. 1, p. 427. Van Nostrand Reinhold, New York, 1992.
10. S. Pei, G. E. Zajac, J. A. Kaduk, J. Faber, B. I. Boyanov, D. Duck, D. Fazzini, T. I. Morrison, and D. S. Young, *Catal. Lett.* **21,** 33 (1993).
11. S. Andersson and A. D. Wadsley, *Nature* **187,** 499 (1960).
12. S. Anderson and A. D. Wadsley, *Acta Chem. Scand.* **15,** 662 (1961).
13. F. D. Hardcastle, H. Klesnar, and C. H. F. Peden, submitted for publication.
14. G. A. Waychunas, *Amer. Mineral.* **72,** 89 (1987).
15. G. E. Brown, Jr., G. Calas, G. A. Waychunas, and J. Petiau, *in* "Spectroscopic Methods in Mineralogy and Petrology" (F. C. Hawthorn, Ed.), Vol. 18, p. 431. Bookcrafters, Chelsea, 1988.
16. J. Mustre de Leon, J. J. Rehr, S. I. Zabinsky, and R. C. Albers, *Phys. Rev. B* **44,** 4146 (1991).
17. S. I. Zabinsky, J. J. Rehr, A. Ankudinov, R. C. Albers, and M. J. Eller, *Phys. Rev. B* (1994).
18. S. Boridga, S. Coluccia, C. Lamberti, L. Marchese, A. Zecchina, F. Buffa, F. Genoni, G. Leofanti, G. Petrini, and G. Vlaic, *J. Phys. Chem.* **98,** 4125 (1994).
19. L. Troger, D. Arvanitis, K. Baberschke, H. Michaelis, U. Grimm, and E. Zschech, *Phys. Rev. B* **46,** 3283.
20. D. H. Lindsley, *in* "Oxide Minerals" (D. Rumble III, Ed.), Vol. 3, p. L-1. Bookcrafters, Chelsea,1976.
21. H. Nyman, M. O'Keefe, and J.-O. Bovin, *Acta Crystallogr.* **34,** 906 (1978).